Effect of soil-conductor gap formation on the fatigue of subsea wellheads

Rafael Dias[1], Anderson Pereira[2]

[1]*CENPES Research Center, PETROBRAS*
Avenida Horácio Macedo, 950, 21941-915, Rio de Janeiro, Brazil
rafael_dias@petrobras.com.br
[2]*Dept. of Mechanical Engineering, Pontifícia Universidade Católica do Rio de Janeiro/PUC-RIO*
R. Marquês de São Vicente, 225, 22451-900, Rio de Janeiro, Brazil
anderson@puc-rio.br

Abstract. Construction and interventions on offshore oil wells in deepwater are usually done by floating rigs. Rig motion is transmitted by the drilling riser to the wellhead and casings, generating fatigue damage on them. We hypothesize that plastic deformation occurs in the soil after emergency disconnections, leaving an open gap between the conductor and soil that changes the dynamical behavior of the system and consequently the accumulated fatigue damage. Two models were developed. The first one is a 3D elastoplastic soil-conductor FEM, where the gap is computed. After that, a global riser analysis with 3D beams is performed. Through numerical experimentation, we found that stiffer soil is more susceptible to the degradation of soil condition, increasing the accumulated damage by about 45 %.

Keywords: Wellhead fatigue, soil-pile gap, soil degradation, riser analysis

Introduction

A Mobile Offshore Drilling Unit (MODU) with dynamic positioning (DP) system floats above the wellhead within a tolerance radius. It must continuously correct its position using thrusters which, like all other rig equipment, are usually powered by diesel-driven generators.

It is possible that the power generation system fails, and the rig begins to drift from the well. The Blowout Preventer (BOP) should be disconnected from the wellhead (WH), but this is a last resort operation, done only when the rig is far enough to damage rig equipment or the wellhead if the generators don't recover from the fault. The Emergency Disconnection System takes some time to hydraulically actuate BOP rams and open the BOP connector, so the rig is farther by the time it stops applying loads to the wellhead.

We expect that the effect of such a high load, especially in deepwater plastic clay, is a permanent deformation of the soil, leaving a gap around the conductor. In the event of a reconnection, soil reaction will be different, and stress distribution along the conductor will change. We aim here to investigate the impact of gap formation on the fatigue damage of the wellhead.

Wellhead Fatigue

Wellhead fatigue is an issue that was poorly explored in the technical literature until the last decade. Very few papers appeared since the first one by Hopper [1] about a fatigue failure on the High-Pressure Housing due to Vortex-Induced Vibration (VIV). The subject matter got more attention when Reinås et al. [2] reported a new well failure in a North Sea field. The investigation of the incident by Statoil and DNV generated a WH fatigue analysis

procedure widely used in industry, later discussed in a JIP and formalized as the recommended practice DNVGL-RP-0142 [3].

The sudden revival of interest in WH fatigue by the industry is probably due to changes driven by the need to operate in ultra-deep environments. As new MODUs were built or upgraded to operate on ultra-deepwater and 3rd generation rigs became less available, interventions and abandonment of old wells with weaker wellhead started to be done with the heavier and taller 6th generation BOP. One example of the consequences was estimated by Greene & Williams [4], where the 3rd generation rig obtained more than 10 times the fatigue life of the 6th generation rig.

Water depth, for example, is another very influential factor. Williams & Purcell [5] obtained an extension of 50 times the fatigue life when going from 100 m to 500 m of water depth. As such, this is one of the parameters we chose to vary in the present study.

Modeling the fatigue accumulation is a complex task, depending on many parameters and whose results are very sensitive to small changes in the input. Of all parameters, soil modeling is one of the biggest sources of uncertainty. First, because soil investigations seldom are done close to the well location. And, even if soil properties are available at the exact location, the proper model for lateral soil-conductor interaction needs to be used. It was recognized by Jeanjean [6] and Zakeri et al [7, 8] that the API RP 2GEO p-y spring model gives an over-conservative estimate of fatigue life, and models that better captured initial stiffness were necessary.

METHODOLOGY

1.1 Gap formation analysis

A 3D finite element analysis of the soil-conductor system is used to quantify the gap formed after the application of a moment load at the wellhead. The geometry of the problem is shown in Fig. 1, along with a view of the wellhead system. The diameter of the conductor casing is 30” (0.762 m) and the wall thickness is 1.5” (0.0381 m). For the surface casing, we considered a 20” x 1” (0.508 x 0.0254 m) casing. Low-pressure and high-pressure housings (LPH and HPH, respectively) were simplified but maintained details of the wellhead landing shoulders. The LPH stickup was fixed to 2.5 m above mudline level, and the casings and soil were modeled up to a depth of 60 m. Horizontal soil limits were extended to 20 times the conductor diameter to minimize the influence of the boundary conditions on the result.

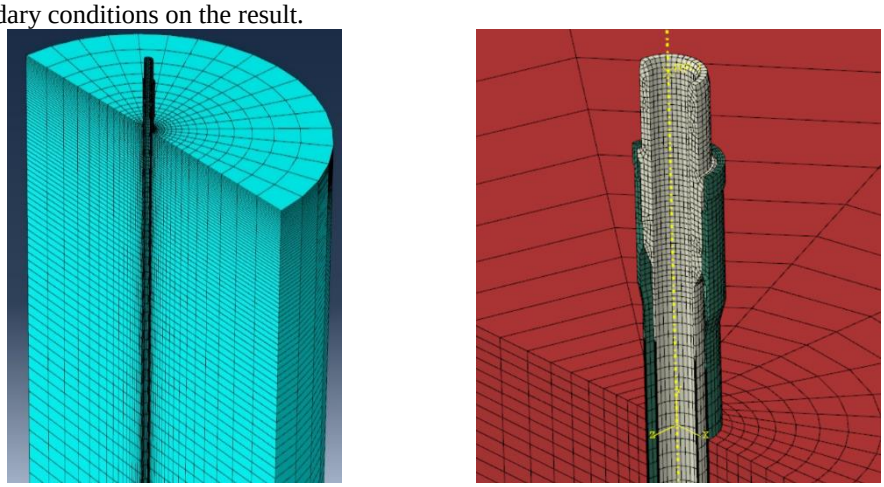

Figure 1. Local model of the wellhead system. Detail of the housings on the right picture.

The conductor and other steel components were modeled by an elastic material, with elastic modulus E = 210 GPa and Poisson’s ratio ν= 0.3. Soil, on the other hand, used an elastic-perfectly plastic constitutive law obeying the Mohr-Coulomb criterion, with the ultimate resistance given by the undrained shear strength S_u, the undrained elastic modulus (E_u) given by a simple correlation (Eq. 1) for soft clays and undrained Poisson’s ration ν_u=0.48, based on a theoretical value of 0.5:

$$E_u = 100 \cdot S_u \tag{1}$$

We chose a 3D linear element with reduced integration (C3D8R) for meshing. Soil mesh was denser near the conductor and seabed surface, with a minimum element size of 0.1 m. Symmetry conditions were applied to have only half of the system modeled. Soil and conductor base were given encastre boundary conditions, while surface casing applied a traction load equivalent to the submerged weight of all the surface casing below the model.

Gap formation was analyzed using a two-steps approach. First, a moment load is applied to the top of high-pressure housing in a quasi-static implicit dynamic step in ABAQUS. Then, the moment is released using another quasi-static implicit dynamic step and permanent deformation of the soil is measured.

1.2 Fatigue analysis

Fatigue analysis is largely based on the procedure of Aronsen et al. [9]. The wellhead loads are obtained through a coupled global riser analysis performed according to ISO 13624-1 standard [10]. Each component of the system is modeled as a cylindrical beam of different equivalent diameters, using the PIPE31H element in ABAQUS [13]. This element provides a three-dimensional, linear Timoshenko beam which includes effects of the external and internal pressure loads. Concentric pipe sections are modeled as one pipe with the same external diameter and thickness to obtain the sum of inertia moment of individual components (Figure 2).

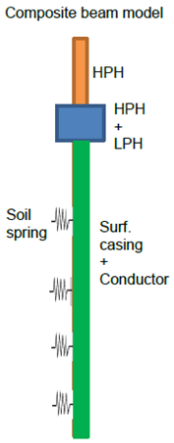

Figure 2. Equivalent beam model for global riser analysis

As for the tensioner system, it was assumed to apply a constant force to the tensioner ring. Lower and Upper Flex Joint used a connector in Abaqus with nonlinear rotational stiffness based on operational limits.

1.3 Vessel movement

Waves cause movement of the vessel in six-degrees-of-freedom (DOF). Each DOF response, given by α_m, is obtained using Eq. 2. The coefficients R_m and φ_m are given by the Response Amplitude Operator (RAO) and depend on the wave amplitude A and wave heading.

$$\alpha_m = R_m \sum_{n=1}^{N} A_n \, cos(\omega_n t + \varphi_n - \varphi_m) \tag{2}$$

In Eq. 2, we used a linear combination of N waves of amplitude A_n, angular frequency ω_n and phase φ_n to describe the resultant wave. This is only possible because a first order wave model was chosen.

For the angular phase φ_n, each wave is assigned a random value in the interval $]-\pi, \pi[$. The wave amplitude is correlated to the wave frequency by $A_n = (2S(\omega)\Delta\omega)^{1/2}$, where $S(\omega)$ is the wave spectrum, that is, the frequency-dependent wave energy. In this work, the JONSWAP wave spectrum was used (Eq. 3). There, H_s is the

significant wave height, f_p and T_p represent the peak frequency and its respective period where the wave energy reaches its maximum.

$$S(\omega) = \beta H_s^2 T_p^{-4} f^{-5} exp\left[\frac{5}{4}\left(\frac{f}{f_p}\right)^{-4}\right]\gamma^{\delta}; \gamma = 3.3; \beta = \frac{0.06328(1.094-0.01915\,ln\,\gamma)}{0.230+0.0336\gamma-\frac{0.185}{1.9+\gamma}}; \sigma = \begin{cases} 0.07\ se\ f < f_p \\ 0.09\ se\ f >= f_p \end{cases};$$
$$\delta = exp\left[-\frac{1}{2}\left(\frac{\frac{f}{f_p}-1}{\sigma}\right)^2\right] \quad (3)$$

1.4 Submerged body loads

The dynamics of submerged bodies consider some additional forces that arise due to fluid-structure interaction. The forced oscillation of a body causes dynamic forces associated with fluid inertia, hydrodynamic damping, and drag. The Morison equation (Eq. 4) is commonly used to approximate these forces in circular cylindrical structures. The resulting force per length in cylinder of diameter D is given by:

$$F = \frac{1}{2}\rho C_D D|v_{rel}|v_{rel} + \rho\frac{\pi D^2}{4}\left(C_M a_f + C_A a_c\right) \quad (4)$$

In Eq. 4 v_{rel} is the relative velocity between the fluid and the structure, a_f and a_c are the accelerations of the fluid and the cylinder, C_D is the drag coefficient, C_A is the added mass coefficient and C_M is the fluid inertia coefficient. These forces were simulated with help of the Abaqus module AQUA.

1.5 Soil reaction

The constitutive model adopted for the soil is of utmost importance for wellhead fatigue. In our global riser analysis, like Aronsen et al. [9], the soil is modeled by non-linear springs, so called p-y formulation. Here, p is the soil pressure and y is the soil displacement. Mercan et al. [11] report that the model of Zakeri et al. [7, 8] gives the best calibration of field data in most cases. The expression for a best fitted p−y curve of normally consolidated clays is:

$$p = 0.67 N_P S_u (y/D)^{0.03}; N_P = 12 - 4\,exp\left(-\zeta(z/D)\right); \zeta = \begin{cases} 0.25 + 0.05\,\lambda\ se\ \lambda = \frac{S_{u0}}{S_{u1}D} < 6.0 \\ 0.55\ se\ \lambda >= 6.0 \end{cases} \quad (5)$$

Here, it is assumed that the shear strength increases linearly with depth, e. g., $S_u = S_{u0} + S_{u1} \cdot z$. A nonlinear spring model is obtained by multiplying the corresponding p-y curve by the conductor projected area $D\Delta z$. These springs are attached to each beam element node in Abaqus.

1.6 Fatigue damage calculation

A sea state is a statistical formulation of the observed sea behavior in a period. For the JONSWAP wave spectrum, it is defined by parameters H_s and T_p. The statistical distribution of sea states can be represented in the wave scatter diagram, where there is the count of each pair of $H_s - T_p$ in a given period.

For simulation purposes, each sea state was assumed to last for 600 s, as recommended by Grytoyr & Steinkjer [12]. An implicit dynamic simulation was run for all of them, obtaining a stress time series over the combined casings.

These stress time series need to be post-processed before using them for fatigue calculations [9]. First, bending moments need to be distributed between the conductor and the surface casing. For depths where the two are cemented together a simple division proportional to the individual inertia moments is enough. In the cases

where the surface casing is uncemented its bending moment distribution (Eq. 6) is estimated by considering it a tensioned beam, with ϕ_1 and ϕ_2 being the top (x = 0) and bottom (x = L) angle.

$$M(x) = M_1\left\{\frac{sinh[k(L-x)]}{sinh(kL)}\right\} + M_2\left[\frac{cosh(kx)}{sinh(kL)}\right];\ M_1 = \frac{\sqrt{TEI}}{A}\phi_1 + M_2\frac{B}{A};\ M_2 = \frac{\sqrt{TEI}(A\phi_2 - B\phi_1)}{B^2 - A^2}$$
$$k = \sqrt{\frac{T}{EI}};\ A = \frac{1}{tanh(kL)} - \frac{1}{kL};\ B = \frac{1}{cosh(kL)} - \frac{1}{kL} \quad (6)$$

After obtaining individual bending moments, fatigue calculations proceed as usual: axial stress is derived for each casing, stress concentration factors are applied at hotspots, rainflow counting is used to get the number of cycles at each stress level, and finally, Miner's rule is applied to calculate total damage of a given sea state. The result is obtained by the weighted average of the damage by the wave scatter diagram.

Results and Discussion

1.7 Gap formation analysis

Our analyses were done for two different soil conditions. The first one represents a normally consolidated clay with a resistance profile given by $S_u = 1.3z + 1$, referred here as the "soft soil", where z is the depth in meters and S_u is given in kPa. The other profile, referred to as the "stiff soil", corresponds to a slightly overconsolidated clay of $S_u = 2.5z + 5$.

The applied load at the bottom of the surface casing was 1.5 MN, equivalent to the floated weight of an 800 m 20" casing, being 600 m immersed on seawater and 200 m immersed on 15.6 ppg (1780 kg/m^3) cement. At the top of the wellhead, a moment equal to the maximum specified load by the manufacturer, 3.25 $MN \cdot m$ was applied. The resulting permanent deformation can be seen in Figure 3. The maximum gap width for the soft soil is 1.7 cm and for the stiff soil is 3.2 mm. As expected, soft soil forms a gap deeper and wider than stiff soils.

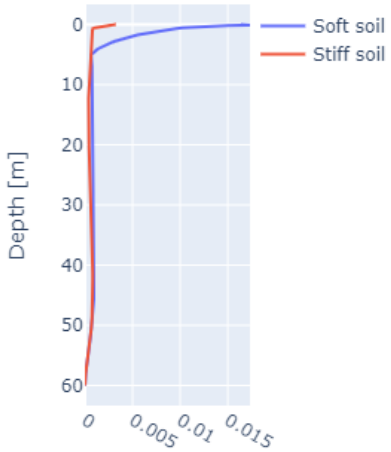

Figure 3. Permanent soil deformation (m) after loading

1.8 Fatigue analysis

First, the effect of soil stiffness is investigated. The base model will be a well in a water depth of 500 m. The riser stack up is given in Table 1, as well as internal and external diameters, floated weight, and hydrodynamical coefficients.

Table 1. Riser stackup

Component	Top [m]	Base [m]	External Radius [m]	Thickness [m]	Floated Weight [kN]	C_A	C_D
Diverter	31.65	28.68	0.781	0.0254	11.640	-	-
UFJ	28.68	28.68	-	-	54.491	-	-
Inner Barrel of Telescopic Joint	28.68	7.05	0.267	0.0159	135.58	-	-
Outer Barrel of Telescopic Joint	7.05	2.60	0.318	0.0254	48.930	-	-
Buoyant Riser Joints	2.60	-271.7	0.689	0.0222	-187.04	1.6	1.0
Bare Riser Joints	-271.7	-481.81	0.270	0.0222	1147.7	1.6	1.5
LFJ	-481.81	-481.81	-	-	100.42	-	-
BOP and LMRP	-481.81	-496.5	1.630	0.3286	2929.6	1.6	5.0
HPH	-496.5	-497.33	0.343	0.1047	19.974	1.6	1.5
HPH and LPH Overlap	-497.33	-498.5	0.454	0.2158	28.155	1.6	1.5
Condutor Casing	-498.5	-560.0	0.381	0.0381	410.17	-	-
Surface Casing	-498.5	-560.0	0.254	0.0254	182.20	-	-

Fatigue damage in two locations with stress concentration is verified. First, for the BOP connector (Figure 4), a greater gap depth allows it to bend with a greater radius of curvature, lowering the bending stress. In the case of soft soil, the influence is barely noticeable, given the low soil reaction that occurs in the initial meters. On the other hand, the stiff soil has more significant results, with a 27% drop in fatigue damage between the intact soil and the one with a gap depth of 2 meters, the maximum value expected by the local simulations.

For the connector of the first conductor joint (Figure 5), this trend is reversed. The presence of a soil gap shifts the maximum bending moment to closer to the conductor connector. For the stiff soil, there is an increase of about 45% damage for a gap depth of 2 meters.

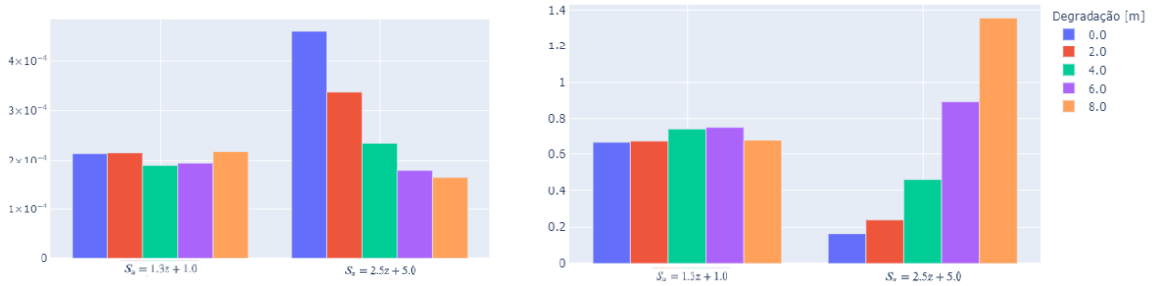

Figure 4 (left) and 5 (right). Fatigue damage variation of BOP connector (Fig. 4) and Conductor connector (Fig. 5) with soil stiffness.

The second assessment we're going to make is related to the water depth. Because fatigue damage on the soft soil was less sensitive to gap depth, we chose to compare the water depths only with the stiff soil. Figure 6 shows the comparison for water depths of 500 m and 2000 m for the BOP connector and Figure 7 shows the same comparison for the conductor connector.

The difference in the order of magnitude between the two water depths is remarkable, being the accumulation of fatigue damage in the deepest water depth two orders of magnitude lesser. This is due to the greater extent of the riser. The displacements imposed by the drilling rig are damped before reaching the wellhead, thus preserving its structure.

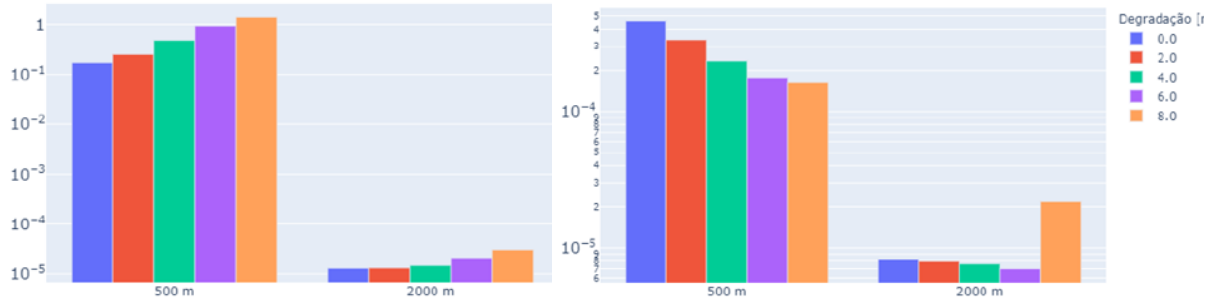

Figure 6 and 7. Fatigue damage variation of BOP (Fig. 6) and Conductor connector (Fig.7) with water depth.

Conclusions

The impact of soil degradation was shown for some combinations of parameters. This soil degradation can have several origins, such as cyclic loading, erosion caused by shallow water flows, or due to the application of a extreme load. The industry's current practice, in these cases, is to evaluate only the mechanical failure of components of the riser-conductor system. However, even if it doesn't happen, the soil is affected and fatigue life changes.

Our global riser analyses were simplified. It remains to study the influence of tensioner system, VIV effect, and using a true cyclic p-y model for effects of a storm load.

Authorship statement. The authors hereby confirm that they are the sole liable persons responsible for the authorship of this work, and that all material that has been herein included as part of the present paper is either the property (and authorship) of the authors, or has the permission of the owners to be included here.

References

[1] C. T Hopper. "Vortex-induced oscillations of long marine drilling riser". In: *Proceedings of Deep Offshore Technology (DOT)*, Valleta, Malta, 1983.
[2] L. Reinås, T. Hørte, M. Sæther, and G. Grytøyr, "Wellhead Fatigue Analysis Method," in *International Conference on Ocean, Offshore and Arctic Engineering*, Rotterdam, The Netherlands: ASMEDC, Jan. 2011, pp. 693–703.
[3] DNV GL AS. "DNVGL-RP-0142: Wellhead fatigue analysis". Det Norske Veritas, Oslo, Norway, 2015.
[4] J. F. Greene and D. Williams, "The Influence of Drilling Rig and Riser System Selection on Wellhead Fatigue Loading," in *International Conference on Ocean, Offshore and Arctic Engineering*, Rio de Janeiro, Brazil: American Society of Mechanical Engineers, Jul. 2012, pp. 621–629. doi: 10.1115/OMAE2012-83754.
[5] D. Williams and K. Purcell, "Optimisation of Conductor System Design to Minimise Wellhead Fatigue Issues," in *International Conference on Ocean, Offshore and Arctic Engineering*, Nantes, France: American Society of Mechanical Engineers, Jun. 2013, p. V04BT04A003. doi: 10.1115/OMAE2013-10829.
[6] P. Jeanjean, "Re-Assessment of p–y Curves for Soft Clays from Centrifuge Testing and Finite Element Modeling," in *Offshore Technology Conference*, Houston, Texas: OTC, May 2009, p. OTC-20158-MS. doi: 10.4043/20158-MS.
[7] A. Zakeri, E. C. Clukey, E. B. Kebadze, and P. Jeanjean, "Fatigue Analysis of Offshore Well Conductors: Part I – Study Overview and Evaluation of Series 1 Centrifuge Tests in Normally Consolidated to Lightly Over-Consolidated Kaolin Clay," *Applied Ocean Research*, vol. 57, pp. 78–95, 2016, doi: 10.1016/j.apor.2016.03.002.
[8] A. Zakeri, E. C. Clukey, E. B. Kebadze, and P. Jeanjean, "Fatigue Analysis of Offshore Well Conductors: Part II – Development of New Approaches for Conductor Fatigue Analysis in Clays and Sands," *Applied Ocean Research*, vol. 57, pp. 96–113, 2016, doi: 10.1016/j.apor.2016.03.001.
[9] K. H. Aronsen, S. Kuzmichev, G. Grytøyr, K. Gregersen, F. Kirkemo, and L. Reinås, "Analysis Approach for Estimating Wellhead Fatigue," in *International Conference on Ocean, Offshore and Arctic Engineering*, Madrid, Spain: American Society of Mechanical Engineers, Jun. 2018, p. V003T02A092. doi: 10.1115/OMAE2018-77214.
[10] ISO. "ISO/TR 13624-2: Petroleum and natural gas industries — Drilling and production equipment— Part 2: Deepwater drilling riser methodologies, operations, and integrity technical report". International Organization for Standardization, Switzerland, december 2009 edition, 2009.
[11] B. Mercan, Y. Chandra, M. Campbell, and M. L. Ge, "Soil Model Assessment for Subsea Wellhead Fatigue Using Monitoring Data," in *Offshore Technology Conference*, Houston, Texas, USA: OTC, May 2017. doi: 10.4043/27662-MS.
[12] G. Grytøyr and O. Steinkjer, "Uncertainty of Long Term Fatigue Load of Subsea Well Heads," in *International Conference on Ocean, Offshore and Arctic Engineering*, Rio de Janeiro, Brazil: American Society of Mechanical Engineers, Jul. 2012, pp. 639–646. doi: 10.1115/OMAE2012-83686.
[13] Dassault Systèmes Simulia Corp. "Abaqus/Standard 2024". Providence, Rhode Island, USA, 2024.